

Influence of barrier thickness on the structural and optical properties of InGaN/GaN multiple quantum wells*

Liang Ming-Ming(梁明明)^{a)b)}, Weng Guo-En(翁国恩)^{a)b)}, Zhang Jiang-Yong(张江勇)^{c)†}, Cai Xiao-Mei(蔡晓梅)^{a)b)}, Lü Xue-Qin(吕雪芹)^{b)}, Ying Lei-Ying(应磊莹)^{c)}, and Zhang Bao-Ping(张保平)^{a)c)‡}

^{a)}Department of Physics, Xiamen University, Xiamen 361005, China

^{b)}Pen-Tung Sah Institute of Micro-Nano Science and Technology, Xiamen University, Xiamen 361005, China

^{c)}Department of Electronic Engineering, Xiamen University, Xiamen 361005, China

(Received 12 August 2013; revised manuscript received 16 October 2013; published online 25 March 2014)

The structural and optical properties of InGaN/GaN multiple quantum wells (MQWs) with different barrier thicknesses are studied by means of high resolution X-ray diffraction (HRXRD), a cross-sectional transmission electron microscope (TEM), and temperature-dependent photoluminescence (PL) measurements. HRXRD and cross-sectional TEM measurements show that the interfaces between wells and barriers are abrupt and the entire MQW region has good periodicity for all three samples. As the barrier thickness is increased, the temperature of the turning point from blueshift to redshift of the S-shaped temperature-dependent PL peak energy increases monotonously, which indicates that the localization potentials due to In-rich clusters is deeper. From the Arrhenius plot of the normalized integrated PL intensity, it is found that there are two kinds of nonradiative recombination processes accounting for the thermal quenching of photoluminescence, and the corresponding activation energy (or the localization potential) increases with the increase of the barrier thickness. The dependence on barrier thickness is attributed to the redistribution of In-rich clusters during the growth of barrier layers, i.e., clusters with lower In contents aggregate into clusters with higher In contents.

Keywords: InGaN/GaN multiple quantum wells, barrier thickness, thermal quenching, localization potential

PACS: 42.70.-a, 78.20.-e, 78.40.Pg, 78.66.Fd

DOI: 10.1088/1674-1056/23/5/054211

1. Introduction

InGaN alloys have attracted much attention for their advantageous bandgap tuning ability of from 3.4 eV for GaN to 0.7 eV for InN, covering nearly the whole wavelength range from blue to near infrared.^[1,2] InGaN/GaN MQWs are widely used as the active layers in high-brightness blue-green light-emitting diodes (LEDs) and continuous wave (cw) laser diodes (LDs).^[3] A great many studies have been done to explore the emission mechanism in InGaN/GaN MQWs.^[4–12] Exciton-localization effect, which is based on “quantum dots” induced by spatial fluctuations of In compositions, has been believed to play an important role in the high performance of InGaN/GaN MQW light emitting devices in spite of the tremendous density of dislocations. A great deal of effort has been devoted to studies of the dependence of the exciton localization on growth parameters such as the well thickness,^[6,7] ramp-up time,^[8] growth temperature,^[9] post-annealing,^[10–12] interruption time between the growth of well and barrier layers,^[13] and so on.

Barrier thickness, which may affect the piezoelectric field in the well,^[14] the carrier transport and distribution in active layers,^[15] the quality of active layers,^[16] and the exciton localization in the well, plays a crucial role in determining the structural and optical qualities of InGaN/GaN MQWs. Understand-

ing the effect of barrier thickness on the InGaN/GaN MQWs is necessary for further improving the performance of the optical devices. Up to now, however, there are only a few reports on the effect of barrier thickness on the exciton localization of InGaN/GaN MQWs. Zheng *et al.*^[17] studied HRXRD and temperature-dependent PL as a function of deposition time of barrier layers. They discussed the possible origin of thermal quenching of the luminescence. However, no further investigations were made into the physical mechanisms responsible for the different optical properties of InGaN/GaN MQWs with different barrier thicknesses.

In this paper, the influence of barrier thickness on the structural and optical properties of InGaN/GaN MQWs is studied. Temperature-dependent PL measurements show that, with the increase of the barrier thickness, not only is the temperature of the turning point from blueshift to redshift of the S-shaped temperature-dependent PL peak energy increased, but also the activation energy of nonradiative recombination process too. In addition, the full width at half maximum (FWHM) of the PL spectra at 12 K is broadened. These results suggest that a thicker barrier (longer growing time) may first cause higher In-content clusters and then enhances the localization effect.

*Project supported by the National Natural Science Foundation of China (Grant Nos. 61106044 and 61274052), the Specialized Research Fund for the Doctoral Program of Higher Education of China (Grant No. 20110121110029), the Fundamental Research Funds for the Central Universities of Ministry of Education of China (Grant No. 2013121024), and the Natural Science Foundation of Fujian Province of China (Grant No. 2013J05096).

†Corresponding author. E-mail: jy Zhang2010@xmu.edu.cn

‡Corresponding author. E-mail: b Zhang@xmu.edu.cn

2. Experiment

All samples were grown on c-plane sapphire substrates by using Thomas Swan low-temperature metalorganic chemical vapor deposition (MOCVD) apparatus. Trimethylgallium (TMGa), trimethylindium (TMIn), and ammonia were used as precursors for Ga, In, and N, while silane (SiH_4) and bis-cyclopentadienyl magnesium (CP_2Mg) were used as n-type and p-type dopants, respectively. Before deposition of a GaN buffer layer, the substrates were treated in a H_2 ambient at 1150°C for 15 min, then a 25-nm-thick low temperature GaN buffer layer was grown and followed by a 2- μm -thick layer of n-GaN. In the following steps, ten pairs of InGaN/GaN MQWs were grown in a nitrogen ambient in order to enhance the indium into the InGaN well layers. The growth temperatures of InGaN wells and GaN barriers were 750°C and 850°C , respectively. For each quantum well pair, we first ramped down the growth temperature to 750°C and waited until the temperature stabilized, and then grew the InGaN well layer for 100 seconds (s). After the growth of the well layer was completed, we ramped the growth temperature up to 850°C and waited again until the temperature stabilized, and then grew the GaN barrier layer for 40 s, 90 s, and 170 s, respectively, for three samples. The ramp-down and ramp-up processes took 250 s and 160 s, respectively, for all the samples. Finally, each sample was capped with a 150-nm p-GaN layer. Three samples, with the same growth conditions and structures except for the barrier thickness, were grown in this study. For simplicity, these samples are denoted by B1, B2, and B3, respectively. The In content of InGaN well layers and the barrier thicknesses of the three samples studied here were determined by the HRXRD and cross-sectional TEM measurements.

PL measurements were performed on the samples held in a helium closed-circuit refrigerator over a temperature range from 12 K to 300 K. The luminescence signal was dispersed by a monochromator and detected by a GaAs photomultiplier tube. A cw semiconductor laser with a wavelength of 405 nm was used for PL excitation.

3. Result and discussion

Figure 1 shows (0002) reflection HRXRD ω - 2θ scans measured from the three samples with different barrier thicknesses. The strongest peaks are from the GaN buffer layers. For the three samples, the spectra show many well-defined satellite (SL) diffraction peaks, reflecting that the interfaces between wells and barriers are abrupt and the entire MQWs region has good periodicity, which is also confirmed by the cross-sectional TEM results of the three samples, as shown in Fig. 2. From the HRXRD and cross-sectional TEM measurements, we obtain that the well width is 3.5 nm and the barrier thicknesses are 6.6 nm, 14.4 nm, and 25.3 nm for samples B1, B2, and B3, respectively. In addition, the In content for all three samples are around 25%.

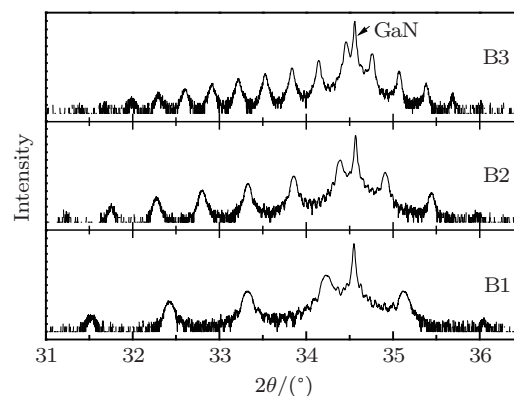


Fig. 1. HRXRD ω - 2θ scans for the (0002) reflection for samples B1, B2, and B3.

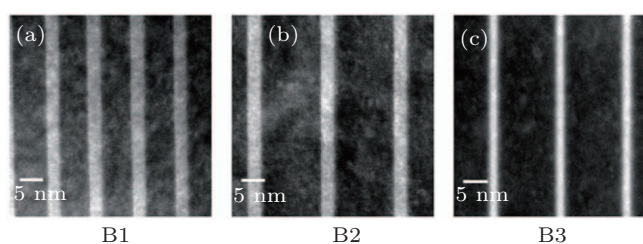


Fig. 2. The cross-sectional TEM images of the InGaN/GaN MQWs region for samples B1 (a), B2 (b), and B3 (c).

To investigate the optical properties of the InGaN/GaN MQWs with different barrier thicknesses, temperature-dependent PL measurement was carried out. The peak energy was plotted against temperature in Fig. 3 and S-shaped (redshift–blueshift–redshift) variation was observed for all samples, which is a commonly known phenomenon. For example, as the temperature increases from 12 K to 60 K, the PL peak of B1 shows a redshift. Then, a blueshift is observed between 60 K and 160 K. When the temperature is further increased to above 160 K, the peak shifts red again. This behavior has been explained as a result of the existence of different localization potential.^[5–9] The possible explanation^[18,19] of the S-shaped temperature dependent behavior of the peak energy is indicated in Fig. 4.

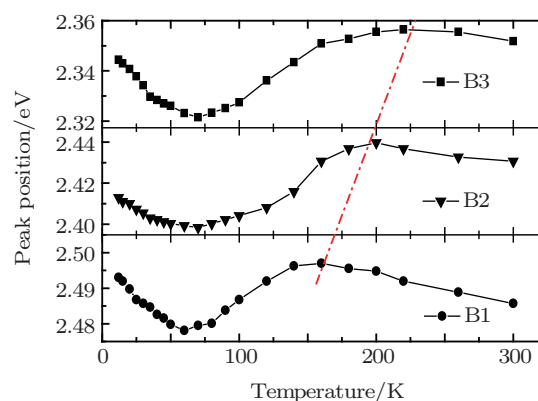


Fig. 3. (color online) The temperature dependence of PL peaks for samples B1, B2, and B3.

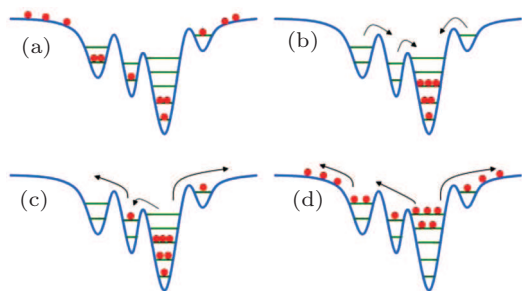


Fig. 4. (color online) Schematic diagrams indicating the possible mechanism of the S-shaped temperature dependent PL peak energy. (a) The distribution of carriers at the lowest temperature where carriers exist in all possible potential minimums, (b) the distribution of carriers at a temperature slightly higher where carriers move to the deepest potential, (c) the distribution of carriers at an even higher temperature where carriers redistribute to higher energies, and (d) the distribution of carriers at very high temperatures where most carriers move out of the localization potentials.

At low temperature, carriers are randomly distributed among the potential minimums (Fig. 4(a)). As the temperature is increased, the carriers localized weakly are thermally activated and have a greater opportunity to relax down into the deeper localization potentials (Fig. 4(b)), which produces a red-shift. By further increasing the temperature, the carriers may have sufficient energy to repopulate the shallow localized states (Fig. 4(c)), thus resulting in the blue-shift of the peak energy. At even higher temperature, most carriers escape from the localized states and become free carriers (Fig. 4(d)). With further increase of the temperature, a red-shift of the peak energy is observed due to the temperature-induced bandgap shrinkage. The temperature of the turning point from blue-shift to red-shift is related to the depth of localization potential. As shown in Fig. 3, the temperature of this turning point of the S-shaped temperature-dependent PL peak energy is 160 K, 200 K, and 220 K for samples B1, B2, and B3, respectively. It means that the localization potential formed by In-rich clusters is deeper for the thicker barrier sample. Therefore, a larger energy is needed for carriers to escape from the localization potential.

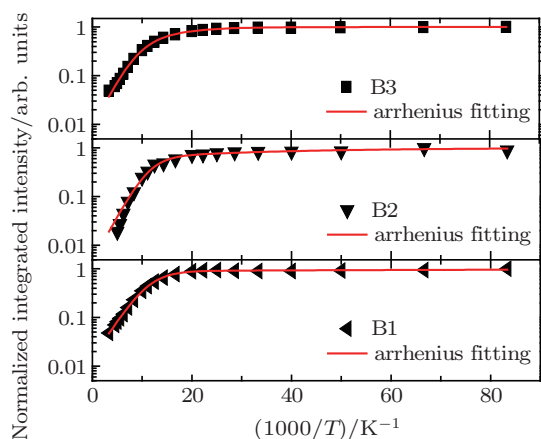


Fig. 5. (color online) Arrhenius plots of the normalized integrated PL intensity for samples B1, B2, and B3 over the temperature ranging from 12 K to 300 K.

Figure 5 shows the Arrhenius plots of the normalized integrated PL intensity for samples B1, B2, and B3 over the temperature range from 12 K to 300 K. Thermal quenching of the normalized integrated PL intensity can be observed for all three samples beginning from about 50 K. In the low temperature range ($T < 50$ K), the integrated PL intensity drops slowly while decreases more rapidly in the high-temperature range ($T > 50$ K). This suggests that there are two different nonradiative recombination processes, corresponding to two different activation energies at these temperature regions. As reported in other papers, the quenching can be explained by thermal emission of the carriers out of a confining potential with an activation energy correlated with the depth of the confining potential.^[19] The following expression considering two nonradiative recombination processes is generally used for calculation of the activation energy in thermally activated processes^[17]

$$I = \frac{1}{1 + A \exp(-E_A/K_0T) + B \exp(-E_B/K_0T)}, \quad (1)$$

where I is the normalized integrated PL intensity as a function of temperature, E_A and E_B are the activation energies of the corresponding nonradiative recombination processes and here the depths of localization potentials, A and B , are constants which are related to the number of defects out of the traps, K_0 is Boltzmann's constant. The fitted parameters are given in Table 1. As can be noticed, the first nonradiative recombination process, which has a larger activation energy E_A , is induced by thermal emission of the carriers out of the deeper potential. In addition, the activation energy E_A increases monotonously with the barrier thickness increasing. It can be seen that the localization potential formed by In clusters is deeper for the thicker barrier samples. For the second one, the activation energy E_B and the constant are very small. This can be related to the escape of carriers captured at the localization minima.^[17,20] In this case, it is easy to understand the thermal quenching of the luminescence process. The second nonradiative recombination process, corresponding to the activation energy, E_B , dominates at the low temperature range. As the temperature is increased from 12 K, most carriers captured at shallow localization potentials could be thermally activated and then relax down into deeper localization potentials and this produces a red-shift of peak energy. Inevitably, some carriers may be captured by defects, resulting in the slowly-dropped integrated PL intensity. With the temperature increasing above 50 K, the first nonradiative recombination process, corresponding to the activation energy E_A , plays a dominant role. Carriers have sufficient energy to redistribute in the localization potentials and even get out of the deep localization potentials with the temperature increasing. It causes a rapid decrease of the integrated PL intensity. For all three samples,

thermal quenching of luminescence becomes much more serious after about 50 K. This temperature is close to the temperature of the turning point from red-shift to blue-shift shown in Fig. 3. These observations are well explained by the analysis above.

Table 1. The fitted results with respect to experimental results of temperature-dependent PL integrated intensities for samples B1, B2, and B3.

	A	E_A/meV	B	E_B/meV
B1	153.8	36.5	0.16	1.4
B2	256.6	39.1	0.83	3.5
B3	786.5	59.3	9	15.6

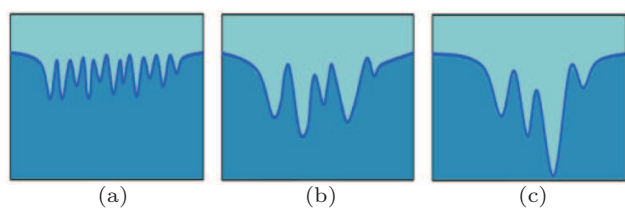


Fig. 6. (color online) Schematic drawings of the energy potentials of In clusters in InGaN wells [(a), (b), and (c)] for samples B1, B2, and B3, respectively.

As is well known, the high indium composition of the In cluster can form the deep localization potential, leading to a lower emission energy and a larger energy escaping from it. Therefore, an In cluster with higher indium composition is formed in the sample with a thicker barrier. Since the only difference between the three samples is the barrier thickness, we can conclude that the change of the In clusters is attributed to the transfer of indium atoms in InGaN wells during the deposition of barrier layers. The thicker barrier needs a longer deposition time. In addition, the growth temperature of GaN barrier layer is higher than that of the well layer. Therefore, this process can be regarded as thermal annealing and the thicker barrier represents a longer thermal annealing time. Doppalapudi *et al.*^[10] studied post annealing on InGaN/GaN MQWs and found that the In-rich dot-like structures would act as nuclei and grow with more annealing time at temperature higher than 725 °C. The growth temperature of the GaN barrier in our study was 850 °C, so an even stronger annealing effect is expected. From this point of view, it is easy to understand the temperature-dependent PL, and a schematic explanation is shown in Fig. 6. In as-grown InGaN well layers, the fluctuation of the indium composition is low and there are only shallow localization centers with low In content. A thin barrier, namely a short annealing time, can hardly change the indium distribution. Thus the shallow localization potentials remain in B1, as shown in Fig. 6(a). As the barrier thickness is increased, the low In content clusters can act as nuclei and aggregate into high In content clusters in B2, as shown in Fig. 6(b). When the barrier thickness is increased further, the accumulation of indium in In clusters is enhanced and the depth of localization

potential induced by the In clusters becomes deeper in B3 as shown in Fig. 6(c). This mechanism can well explain that the localization potential formed by In clusters is deeper for the thicker barrier samples.

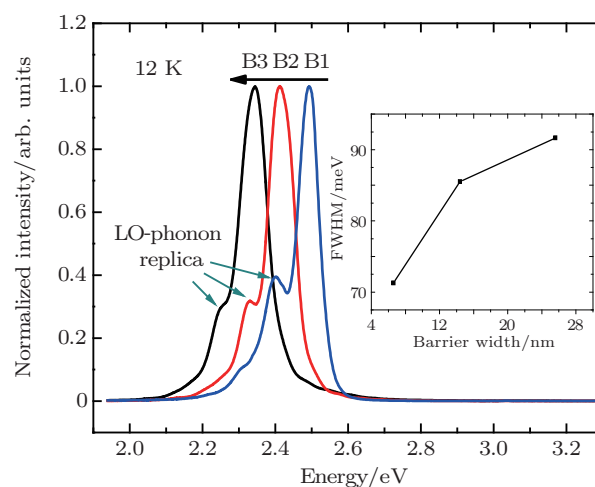


Fig. 7. (color online) Normalized PL spectra of samples B1, B2, and B3 at 12 K and the inset shows the FWHM of these samples.

This result is also confirmed by low-temperature PL measurements. Figure 7 depicts the normalized PL spectra and the linewidths of samples B1, B2, and B3 at 12 K. The linewidths of B3 and B2 are larger than that of B1, which can be easily explained by the cluster model discussed above. Enhancements of composition inhomogeneity of In clusters resulted in the broadening of emission spectra for B2 and B3. In this case, the localization potential formed due to In clusters is deeper for the thicker barrier samples.

It is noted that McCluskey *et al.*^[11] drew a converse conclusion that outdiffusion of the In-rich regions into the surrounding matrix and interdiffusion between InGaN/GaN heterojunctions may occur simultaneously at annealing temperature as high as 1400 °C. In this case, both the In-fluctuation and the maximum In composition are expected to decrease greatly. This is obviously not the case we found. The reason is that the growth temperature (850 °C) of the barrier (or the annealing temperature) is much lower in our study.

4. Conclusion

In summary, we investigated the effect of barrier thickness on structural and optical properties of InGaN/GaN MQWs structures by HRXRD, cross-sectional TEM, and temperature-dependent PL. The ω - 2θ scans of (0002) reflection and cross-sectional TEM measurements showed that the interfaces between wells and barriers were abrupt and the entire MQWs region had good periodicity for samples B1, B2, and B3. Temperature-dependent PL indicated that the localization potential formed by In clusters is deeper for the thicker barrier sample. A mechanism associated with In-accumulation

under thermal annealing could explain this well. The thicker barrier needs a longer deposition time and this process was similar to a thermal annealing. As the barrier thickness was increased, the low In content clusters could act as nuclei and aggregated into high In content clusters, and the localization potential due to in In-rich clusters became deeper. Since the barrier thickness strongly affects the structural and optical properties of InGaN/GaN quantum-well structures, the results presented in this article is important in designing InGaN/GaN-based optical devices.

References

- [1] Matsuoka T, Okamoto H, Nakao M, Harima H and Kurimoto E 2002 *Appl. Phys. Lett.* **81** 1246
- [2] Jain S C, Willander M, Narayan J and van Oberstraeten R 2000 *J. Appl. Phys.* **87** 965
- [3] Nakamura S and Chichibu S F 2000 *Introduction to Nitride Semiconductor Blue Lasers and Light Emitting-Diodes* (New York: Taylor & Francis) pp. 153–165
- [4] Cao W Y, He Y F, Chen Z, Yang W, Du W M and Hu X D 2013 *Chin. Phys. B.* **22** 076803
- [5] De S, Layek A, Raja A, Kadir A, Gokhale M R, Bhattacharya A, Dhar S and Chowdhury A 2011 *Adv. Funct. Mater.* **21** 3828
- [6] Bai J, Wang T and Sakai S 2000 *J. Appl. Phys.* **88** 4729
- [7] Chen X, Zhao B J, Ren Z W, Tong J H, Wang X F, Zhuo X J, Zhang J, Li D W, Yi H X and Li S T 2013 *Chin. Phys. B.* **22** 078402
- [8] Wang Y, Pei X J, Xing Z G, Guo L W, Jia H Q, Chen H and Zhou J M 2007 *J. Appl. Phys.* **101** 033509
- [9] Olaizola S M, Pendlebury S T, O'Neill J P, Mowbray D J, Cullis A G, Skolnick M S, Parbrook P J and Fox A M 2002 *J. Phys. D: Appl. Phys.* **35** 599
- [10] Doppalapudi D, Basu S N, Ludwig K F J and Mousakas T D 1998 *J. Appl. Phys.* **84** 1389
- [11] McCluskey M D, Romano L T, Krusor B S, Bour D P, Johnson N M and Brennan S 1998 *Appl. Phys. Lett.* **72** 1730
- [12] Li Z H, Yu T J, Yang Z J, Feng Y C, Zhang G Y, Gao B P and Niu H B 2005 *Chin. Phys.* **14** 830
- [13] Cheong M G, Yoon H S, Choi R J, Kim C S, Yu S W, Hong C H, Suh E K and Lee H J 2001 *J. Appl. Phys.* **90** 5642
- [14] Hu X L, Zhang J Y, Shang J Z, Liu W J and Zhang B P 2010 *Chin. Phys. B* **19** 117801
- [15] Liu J P, Ryou J H, Dupuis R D, Han J, Shen G D and Wang H B 2008 *Appl. Phys. Lett.* **93** 021102
- [16] Kim D J, Moon Y T, Song K M and Park S J 2001 *Jpn. J. Appl. Phys.* **40** 3085
- [17] Zheng X H, Chen H, Yan Z B, Li Z S, Yu H B, Huang Q and Zhou J M 2004 *J. Appl. Phys.* **96** 1899
- [18] Wang H N, Ji Z W, Qu S, Wang G, Jiang Y Z, Liu B Y, Xu X G and Mino H 2012 *Opt. Express* **20** 3932
- [19] Cho Y H, Gainer G H, Fischer A J, Song J J, Keller S, Mishra U K and DenBaars S P 1998 *Appl. Phys. Lett.* **73** 1370
- [20] Hao M, Zhang J, Zhang X H and Chua S 2002 *Appl. Phys. Lett.* **81** 5129